Cytochrome rC_{552}, Formed during Expression of the Truncated, *Thermus thermophilus* Cytochrome c_{552} Gene in the Cytoplasm of *Escherichia coli*, Reacts Spontaneously To Form Protein-Bound 2-Formyl-4-vinyl (*Spirographis*) Heme[†,‡]

James A. Fee,[*,§,||] Thomas R. Todaro,[§] Eugene Luna,[§] Donita Sanders,[§] Laura M. Hunsicker-Wang,[§,||] Kirti M. Patel,[⊥] Kara L. Bren,[⊥] Ester Gomez-Moran,[@] Michael G. Hill,[@] Jingyuan Ai,[#] Thomas M. Loehr,[#] W. Anthony Oertling,[+] Pamela A. Williams,[||,●] C. David Stout,[||] Duncan McRee,[||,◆] and Andrzej Pastuszyn[○]

Department of Biology, University of California at San Diego, La Jolla, California 92093, Department of Molecular Biology, The Scripps Research Institute, La Jolla, California 92037, Department of Chemistry, University of Rochester, Rochester, New York 14627-0216, Department of Chemistry, Occidental College, Los Angeles, California 90041, Department of Environmental and Biomolecular Systems, OGI School of Science and Engineering, Oregon Health and Science University, Beaverton, Oregon 97006-8921, Department of Chemistry/Biochemistry, Eastern Washington University, Cheney, Washington 99004, and Department of Biochemistry and Molecular Biology, University of New Mexico, Albuquerque, New Mexico 87131-5221

Received May 20, 2004; Revised Manuscript Received July 13, 2004

ABSTRACT: Expression of the truncated (lacking an N-terminal signal sequence) structural gene of *Thermus thermophilus* cytochrome c_{552} in the cytoplasm of *Escherichia coli* yields both dimeric (rC_{557}) and monomeric (rC_{552}) cytochrome *c*-like proteins [Keightley, J. A., *et al*. (1998) *J. Biol. Chem. 273*, 12006−12016], which form spontaneously without the involvement of cytochrome *c* maturation factors. Cytochrome rC_{557} is comprised of a dimer and has been structurally characterized [McRee, D., *et al*. (2001) *J. Biol. Chem. 276*, 6537−6544]. Unexpectedly, the monomeric rC_{552} transforms spontaneously to a cytochrome-like chromophore having, in its reduced state, the $\mathbf{Q_{00}}$ transition (α-band) at 572 nm (therefore called p572). The X-ray crystallographic structure of rC_{552}, at 1.41 Å resolution, shows that the 2-vinyl group of heme ring I is converted to a [heme-CO-CH_2-S-CH_2-C_α] conjugate with cysteine 11. Electron density maps obtained from isomorphous crystals of p572 at 1.61 Å resolution reveal that the 2-vinyl group has been oxidized to a formyl group. This explains the lower energy of the $\mathbf{Q_{00}}$ transition, the presence of a new, high-frequency band in the resonance Raman spectra at 1666 cm^{-1} for oxidized and at 1646 cm^{-1} for reduced samples, and the greatly altered, paramagnetically shifted ^1H NMR spectrum observed for this species. The overall process defines a novel mechanism for oxidation of the 2-vinyl group to a 2-formyl group and adds to the surprising array of chemical reactions that occur in the interaction of heme with the CXXCH sequence motif in apocytochromes *c*.

Cytochrome *c* synthesis in Gram-negative prokaryotes normally occurs from a messenger RNA that encodes a pre-apoprotein having a short (∼20 amino acids) N-terminal signal peptide. The latter is recognized by the general secretory pathway which directs the pre-apoprotein to the periplasm. The signal peptide is further recognized by leader peptidases that cleave it to form apocytochrome *c*. Heme is also synthesized in the cytoplasm and transferred to the periplasm with assistance from still unidentified factors. Apoprotein and heme are thus brought together in the periplasm with the correct rotational orientation of the heme maintained, and additional Ccm[1] factors assist in the correct formation of two thioether linkages with the common CXXCH sequence motif. The *Escherichia coli* system has been extensively reviewed by Thöny-Meyer (*1*, *2*), Kranz (*3*), and Ferguson (*4*) and their co-workers.

[†] Supported by NIH Grants GM35342 (J.A.F.), GM18865 (T.M.L.), GM63170 (K.L.B.), and GM48495 (C.D.S.).

[‡] Structure coordinates of cytochromes rC_{552} and p572 were deposited with the Protein Data Bank as entries 1QYZ and 1ROQ, respectively.

* To whom correspondence should be addressed. Telephone: (858) 784-9235. Fax: (858) 784-2857. E-mail: jafee@scripps.edu.

[§] University of California at San Diego.

[||] The Scripps Research Institute.

[⊥] University of Rochester.

[@] Occidental College.

[#] Oregon Health and Science University.

[+] Eastern Washington University.

● Present address: Astex Technology, 436 Cambridge Science Park, Cambridge CB4 OQA, United Kingdom.

◆ Present address: ActiveSight, 4045 Sorrento Valley Blvd., San Diego, CA 92121.

[○] University of New Mexico.

[1] Abbreviations: BCA, bicinchoninic acid; Ccm, cytochrome *c* maturation; rsC_{552}, recombinant cytochrome *c* obtained from the expression of the chimeric *Thermus versutus*/*T. thermophilus cycA* gene in *E. coli* cells also bearing plasmid pEC86; rC_{552}, monomeric species of recombinant cytochrome *c* obtained from the expression of the truncated *T. thermophilus cycA* gene in *E. coli*; p572, product obtained from the spontaneous transformation of rC_{552} at elevated temperatures and characterized by a $\mathbf{Q_{00}}$ transition at 572 nm in the reduced form; rC_{557}, minor species of recombinant cytochrome *c* obtained from the expression of the truncated *T. thermophilus cycA* gene in *E. coli* and characterized by a $\mathbf{Q_{00}}$ transition at 557 nm in the reduced form and a disulfide-bridged dimeric structure; rR, resonance Raman.

10.1021/bi048968l CCC: $27.50
Published on Web 09/02/2004

In a number of cases, expression in the *E. coli* cytoplasm of truncated cytochrome *c* genes (those lacking the code for the signal peptide) yields an apocytochrome *c* that folds normally and binds heme correctly (*5*−*12*). For example, the truncated gene for *Hydrogenobacter thermophilus* cytochrome *c* yields a protein with correct thioether linkages, apparently due to the correct proximity of protein thiol and heme vinyl entities, and proper folding (*5*−*12*). For other cytochromes *c*, however, cytoplasmic apocytochrome either is degraded or aggregates, and no holocytochrome *c* is formed (*13*). In the case of the truncated *Thermus thermophilus* cytochrome c_{552} gene, expression in *E. coli* leads to incompletely or incorrectly formed versions of the protein that reveal novel heme−protein interactions.

The *T. thermophilus* cytochrome c_{552} was first described by Hon-Nami in 1977 (*14*). When its truncated structural gene was placed under control of the T7 RNA polymerase promoter in a plasmid borne by *E. coli*, the cells became distinctly red in color (*15*). This simple observation suggested the synthesis of abundant amounts of holocytochrome *c*. Purification, however, yielded dimeric rC_{557} and monomeric cytochrome rC_{552} (*11*) (see below). X-ray structure analysis yielded the novel findings that rC_{557} is comprised of cytochrome monomers in which the heme moeity is "flipped" about its $\alpha-\gamma$ axis, cysteine 14 has formed a thioether linkage with the 2-vinyl rather than the 4-vinyl group, the 2-vinyl group remains unreacted, and a disulfide has formed between the monomers by oxidation of the two Cys11 residues (*16*). This finding is important to the development of expression systems for cytochromes *c*.

Recently, there have been significant advances in the development of molecular genetic, expression systems for obtaining useful quantities of native-like cytochromes *c*. These are needed to address the roles of these proteins in energy metabolism, mechanisms of electron transfer, protein control of redox potentials, protein folding, apoptosis, etc. These and related efforts continue to be limited by the availability of large quantities of native-like, recombinant proteins (see ref *17* for discussion).

E. coli is a natural choice for the development of an expression system. The first of these involved plasmid-directed expression of yeast (*Saccharomyces cerevisiae*) 1-isocytochrome *c* in the cytoplasm of *E. coli* (*10*). Originally, the 1-isocytochrome *c* structural gene was tandemly expressed with the yeast cytochrome *c* (heme) lyase gene and produced ∼15 mg of mature 1-isocytochrome *c* per liter of culture medium. The material was spectrally identical to native protein, but Lys72 was not trimethylated, as occurs in yeast cells. A variation on this system (*17*), in which the yeast heme lyase gene was tandemly expressed with the structural gene for horse heart cytochrome *c*, gave yields of native-like protein as high as ∼100 mg per liter of culture medium. Unfortunately, the yeast heme lyase does not recognize prokaryotic apocytochromes *c* (*18*).

An alternative expression protocol, though not as quantitatively dramatic, has been to insert code for a signal peptide upstream of the cytochrome *c* structural code, which leads to transport of the pre-apocytochrome into the *E. coli* periplasm. Coexpression of periplasm-directed Ccm factors, from an independently propagated plasmid (*19*), has been found to yield modest but useful amounts (≈1 mg per liter of culture medium) of soluble, native-like cytochromes *c* from *Paracoccus denitrificans* (*20*) and *T. thermophilus* (*21*). It has been noted that this system has a much broader range of acceptable pre-apoproteins (*18*).

None of these systems is perfect, however, and their development continues. As noted by Rumbley *et al*. (*17*), there are issues of folding traps, fidelity of heme insertion, and possibly incorrect chemical interaction of heme with the CXXCH residues. Our previous work on the expression of the truncated version of the *T. thermophilus* cytochrome *c* gene showed that at least two "near" cytochromes actually form in the absence of assistance from maturation factors (*11*). Heme inversion (*16*) is now recognized as a common error of cytochrome *c* synthesis in the *in vitro* reaction of heme with apocytochromes *c* (*13*, *22*, *23*) and *in vivo* in the case of the Lys8Gly mutant form of horse cytochrome *c* (*17*), despite the presence of the heme lyase. It is reasonable that knowledge of other, unexpected interactions between the two thiol groups of the apocytochrome *c* and the two vinyl groups of the heme, as reported here, is important for understanding correct cytochrome *c* synthesis.

EXPERIMENTAL PROCEDURES

Recombinant Cytochromes. The cytochrome *c* notation, origin, and defining properties are presented in footnote 1. Native-like cytochrome c_{552}, called rsC_{552}, was obtained as described by Fee *et al*. (*21*). Monomeric, recombinant cytochrome rC_{552}, which is the starting material for this work, was prepared from aerobically grown *E. coli* cells as described by Keightley *et al*. (*11*) and freed of dimeric, recombinant rC_{557} as described by McRee *et al*. (*16*). The p572 forms spontaneously from cytochrome rC_{552} and can be purified as follows. Approximately 5 mg of purified rC_{552} was exchanged into 50 mM sodium phosphate buffer at pH 7.0 (solution A) and heated in a sealed Eppendorf tube at ∼70 °C for 1 h. The protein was then loaded onto a 5 mL, cation-exchange column (Amersham-Pharmacia Mono S) and developed as follows: 0−20 mL of 0% solution B, 20−60 mL of 0−50% solution B, and 60−95 mL of 50−100% solution B. Solution B is solution A with 0.1 M NaCl. Fractions (1 mL) were collected. Most of the cytochrome elutes between ∼15 and 35% solution B, although small amounts of cytochrome elute throughout the elution profile. The pattern is variable from sample to sample and quite complex. Optical spectra of each fraction were recorded in oxidized and reduced states, and spectrally pure p572 was usually found near 25 mL (25% solution B). Other fractions contained mixtures of p572 and rC_{552}. Fractions largely free of rC_{552} were combined and concentrated for use in various experiments. Chromatography on a Vydac 201TP54 reverse-phase column under denaturing conditions shows a single sharp band in the elution profile (see below). The chromophore is stable to the usual laboratory manipulation. BCA protein analyses suggest $\epsilon^{red}_{572} = 22\,400\ M^{-1}\ cm^{-1}$, and this value is used throughout to determine p572 concentration.

General Methods. Optical absorption spectra were recorded on a SLM.AMINCO model DB3500 spectrophotometer in 1 cm cells. Fully oxidized proteins were obtained by adding potassium ferricyanide to a final concentration of 10 μM, and reduced proteins were prepared by additions of minute amounts of solid sodium dithionite to the optical cuvette and thorough mixing. The reduced minus oxidized extinction coefficient [$\Delta\epsilon = 14.3\ mM^{-1}\ cm^{-1}$ (*14*)] was used

Table 1: Data and Refinement Statistics for Recombinant *Thermus* Cytochromes rC_{552} and p572[a]

	p572	rC_{552}
X-ray wavelength (Å)	0.978	0.92017
SSRL beamline	9−1	9−1
no. of reflections	126687	80045
no. of unique reflections	17825	31680
R_{merge} (%)	8.5 (30−1.61 Å resolution)	6.6 (30−1.41 Å resolution)
R_{merge} (%)	42.0 (1.64−1.61 Å resolution)	35.6 (1.45−1.41 Å resolution)
completeness (%)	98.9 (30−1.61 Å resolution)	94.3 (30−1.41 Å resolution)
completeness (%)	98.9 (1.65−1.61 Å resolution)	98.6 (1.45−1.41 Å resolution)
multiplicity	7.1	5.5
I/σ_i	7.7 (30−1.61 Å resolution)	5.5 (30−1.41 Å resolution)
I/σ_i	2.2 (1.65−1.61 Å resolution)	2.1 (1.45−1.41 Å resolution)
R-factor ($I > 4\sigma$) (%)	17.1	17.8
R-factor ($I > 0$) (%)	18.7	19.7
R_{free} ($I > 4\sigma$) (%)	23.0	23.5
R_{free} ($I > 0$) (%)	25.5	26.0
rmsd for bonds (Å)	0.01	0.015
rmsd for angle distances (Å)	0.02	0.025

[a] The space group is $p6_5$. $\alpha = 90°$. $\beta = 90°$. $\gamma = 120°$. For rsC_{552}, $a = b = 86.90$ Å and $c = 31.85$ Å. For rC_{552}, $a = b = 87.46$ Å and $c = 32.21$ Å. For p572, $a = b = 86.77$ Å and $c = 31.84$ Å.

to determine approximate concentrations of rC_{552}. Pyridine hemochromes were prepared according to the method of Berry and Trumpower (*24*). The level of protein was measured by the BCA protein assay kit of Pierce according to manufacturer's directions. Cytochrome *c* oxidase activity, using *Thermus* cytochrome ba_3 purified by the method of Keightley *et al*. (*25*), was determined polarographically at 25 °C using an Instech (Plymouth Meeting, PA) unit with output to a strip chart recorder.

X-ray Crystallography. Crystals of rC_{552} (4 °C) and p572 (room temperature), being isomorphous with those of rsC_{552}, were obtained in sitting drops against 36% MPEG 5K (w/w), 0.2 M imidazole malate buffer (pH 6.3) using ~12 mg/mL protein suspended in 25 mM Tris-HCl (pH 8.0) and 100 mM NaCl (see ref *21*). Cryoprotection of crystals was achieved by transferring them to mother liquor supplemented with 20% glycerol. Diffraction data were collected at 100 K at the Stanford Synchrotron Radiation Laboratory (SSRL) to a resolution of 1.41 Å for rC_{552} and 1.61 Å for p572 (see Table 1). The primary data were processed using MOSFLM (*26*), scaled, and further reduced using the CCP4 suite of programs (*27*) (see Table 1). Initial electron density maps were generated using the native and recombinant structures (*21*, *28*) (PDB entries 1C52 and 1DT1) and interpreted further using XtalView (*29*). The model was refined in successive rounds using SHELXL (*30*, *31*) with a test set of 5% randomly chosen reflections being used to calculate R_{free} at each stage. X-ray amplitudes, phases, and derived atomic coordinates have been deposited with the Protein Data Bank (PDB entry 1QYZ for rC_{552} and PDB entry 1ROQ for p572). Heme atoms are referenced in both PDB notation and that found in Falk (*32*).

Protein Chemistry. Pepsin digestion was carried out with a 2 mg/mL stock pepsin solution in 5% formic acid according to the methods of Smyth (*33*). Holocytochrome *c* (0.78 mg) was dissolved in 0.66 mL of 5% formic acid, and a pepsin (CalBiochem) solution was added to a final w/w ratio of 10:1. This mixture was incubated at 37 °C for 22 h followed by drying with *in vacuo* centrifugation. The dried samples were redissolved in 0.1% TFA in water and applied to a Vydac 201TP54 column, and a 5 to 65% acetonitrile gradient, in the presence of 0.1% TFA, was used to elute the peptides. The eluant was monitored at both 400 and 214 nm, and the heme-containing peptide was subsequently characterized by mass spectrometry. It is noteworthy that these compounds are unstable and decompose over the course of a few weeks even when dry at −20 °C.

Mass Spectrometry. Electrospray mass spectrometry of proteins was carried out at the Scripps Research Center for Mass Spectrometry (La Jolla, CA) using a Perkin-Elmer API 100 Sciex single-quadrupole mass analyzer with the orifice potential set at 100 V. Mass spectra were obtained from ion spectra using the Perkin-Elmer program BioMultiView. MALDI-TOF experiments were carried out using a PerSeptive spectrometer. Matrix-assisted laser desorption/ionization (MALDI) FTMS experiments were performed on an IonSpec FTMS mass spectrometer (see ref *34*).

CD Spectroscopy. Samples of oxidized rC_{552} or rsC_{552} for circular dichroism (CD) spectroscopy were 10 μM in protein (for far-UV spectra) or 100 μM in protein (for Soret region spectra) in 100 mM potassium phosphate buffer (pH 7.0). CD spectra were recorded on a JASCO J-710 spectropolarimeter at 22 °C on samples in a quartz cell with a path length of 0.1 cm.

Resonance Raman. Spectra were obtained using a custom McPherson 2061/207 spectrograph (focal length of 0.67 m with a 2400 groove/mm grating), a Princeton Instruments liquid N_2-cooled (LN-1100PB) CCD detector, and a Kaiser Optical holographic super-notch filter. Excitation (413 nm, 5 mW) came from a Coherent Innova 302 Kr laser. Spectra collected in a 90°-scattering geometry for 5 min at room temperature were obtained from 10 μL samples [protein concentration of 20−30 μM in 100 mM Tris-HCl buffer (pH 8)] in glass capillaries. Frequencies, accurate to 1 cm^{-1}, were calibrated relative to indene. Princeton Instruments' WinSpec software was used for data acquisition. Exported ASCII-xy files were analyzed using GRAMS-386 software (Galactic Industries).

NMR Spectroscopy. Protein samples for ^1H NMR spectroscopy were 0.25−1.5 mM in protein in 100 mM potassium phosphate (pH 7.0) in 90% D_2O. Samples were oxidized with a 3-fold excess of potassium ferricyanide and concentrated using a Centricon-10 device prior to data collection. NMR spectra were collected on a 500 MHz Varian INOVA instrument at 25 °C and using a recycle time of 250 ms. Spectra were processed with 30 Hz line broadening.

Electrochemistry. Electrochemical experiments were carried out in a three-compartment cell using a Bioanalytical Systems (BAS) model CV 50W electrochemical analyzer. The gold-disk working electrode was polished with 0.05 μm aluminum oxide (Buehler), thoroughly rinsed, and then chemically modified by sonication for 30 min in a 0.05 mM aqueous solution of pyridine 4-aldehydesemicarbazone. Potentials were measured versus a standard calomel electrode. The reference electrode was separated from the working compartment by a Luggin capillary. Data were recorded at a pyridine 4-aldehydesemicarbazone-modified

gold electrode with a scan rate of 25 mV/s. Both native and recombinant cytochromes gave linear plots of peak current versus (scan rate)$^{1/2}$, consistent with a diffusion-controlled process. Approximately 20% of the rC_{552} sample was converted to p572 (as confirmed by visible spectroscopy), resulting in a shoulder in the voltammogram at ~325 mV. The protein concentrations were ~0.3 mM for p572 and the 1:1 rC_{552}/p572 mixture, and ~1 mM for rsC_{552} in 100 mM potassium phosphate buffer (pH 7).

RESULTS

Formation and Purification of p572

The as-isolated rC_{552} spontaneously converts to a material having an absorption band at 572 nm unless maintained at cold-room temperatures. This occurs upon standing at room temperature for several days or by heating at elevated temperatures for a few minutes. Addition of ferricyanide causes this peak to disappear, and subsequent addition of dithionite results in reappearance of the 572 nm band as well as a significantly attenuated 552 nm band. Additional experiments revealed that neither dioxygen nor light is required and that one-electron, reduced rC_{552} was converted to p572 with equal efficiency (not shown). Figure 1A shows the UV (left panel) and visible (right panel) optical absorption spectra of purified rC_{552} in the oxidized (traces i, dotted line) and reduced (traces i, solid line) states. Formation of p572 was started with fully oxidized rC_{552} by heating for 30 min at 70 °C.[2] After heating had been carried out, the spectrum changed to that shown as the thick solid line in Figure 1A (trace ii). Addition of a slight molar excess of ferricyanide yielded the bottom dotted line in Figure 1A (traces iii), and subsequent addition of excess dithionite gave the bottom solid line in Figure 1A (traces iii), indicating a mixture of reduced rC_{552} and reduced p572. These observations suggest that some portion of the as-isolated rC_{552} spontaneously converts to a new form of iron porphyrin. Appearance of the reduced form of p572 probably results from the presence of spurious reductants in the solution rather than reduced p572 being a mechanistic requirement (see below). Such behavior has been observed in other high-potential metalloproteins (*35*).

It is possible to purify p572 from the remaining rC_{552} by cation exchange, possibly because only the p572 is in the one-electron reduced form and therefore has a different overall charge than the residual cytochromes *c* (see ref *36*); details are provided in Experimental Procedures. With this technique, we prepared ~1 mg quantities of pure p572 for characterization. Evidence of purity includes a single peak on reversed-phase liquid chromatography, a single band upon sodium dodecyl sulfate−polyacrylamide gel electrophoresis

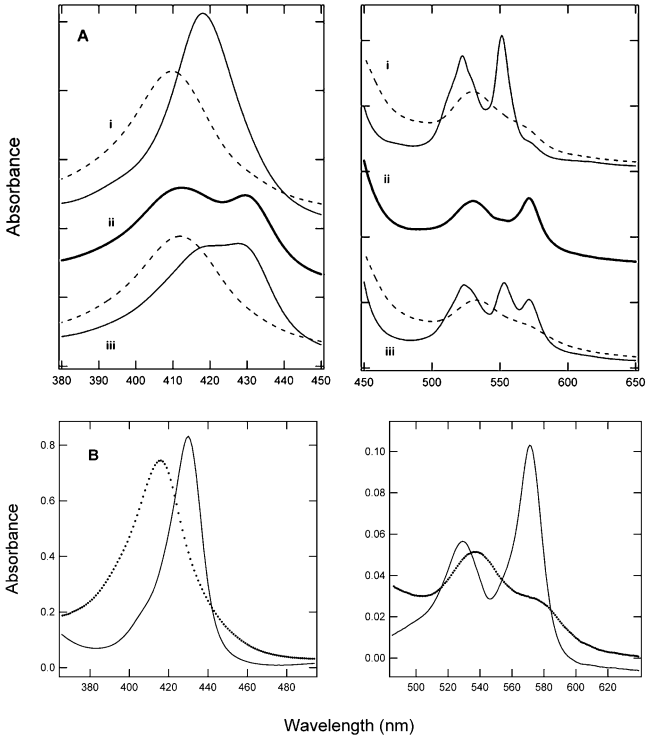

FIGURE 1: (A) Effects of heating on the optical absorption spectra of recombinant *T. thermophilus* cytochrome rC_{552}. The Soret region is shown in the left panel and the visible region in the right panel (5-fold vertical expansion). Sets of traces relating to a single experiment are offset to accommodate all spectra in one presentation. (i) Oxidized (- - -) and reduced (—) spectra of the as-isolated cytochrome rC_{552}. A small amount of p572 is already evident in this sample. (ii) Spectrum after heating the oxidized form of as-isolated rC_{552} for 30 min at 70 °C and cooling to room temperature. (iii) After heating, the solution having the spectrum shown in trace ii was treated with a small molar excess of ferricyanide to obtain the oxidized spectrum of the heated solution (- - -). An excess of sodium dithionite was subsequently added to obtain the reduced spectrum (—) of the heated solution, which reflects a mixture of rC_{552} and p572. The pH was 8.0 in a 50 mM Tris-HCl buffer containing 0.1 M NaCl. (B) Optical absorption spectra of purified p572. The Soret region is shown in the left panel and the visible region in the right. The oxidized spectrum (- - -) was obtained in the presence of a small excess of ferricyanide, and the reduced spectrum (—) was obtained by subsequently adding a small excess of dithionite. The concentration of the sample was ~5 μM. See Table 2 for the visible region extinction coefficient.

(data not shown), electrospray mass spectrometry (see below), and formation of single crystals suitable for X-ray crystallographic studies (see below). To quantify p572, we determined that the 572 nm absorption band has a molar absorbance ϵ^{red}_{572} of ≅22400 M^{-1} cm^{-1} (see Experimental Procedures). Table 2 lists relevant absorption bands and available extinction coefficients for the different proteins used in this study. These preliminary observations suggest that p572 is a modified cytochrome *c* that retains electron transfer competency.

Figure 1B shows optical absorption spectra of purified, oxidized, and reduced p572, and Table 2 lists quantitative data. The spectrum of the oxidized form differs little from that of oxidized rC_{552}, whereas the reduced protein is significantly different. The shift of the $\mathbf{Q_{00}}$ transitions to lower energy in p572 would be consistent with the presence of a carbonyl or Schiff base coupled to the porphyrin π-system, as occurs in heme A-containing proteins (refs *37* and *38* and references therein). Hints of this came with the

[2] The appearance of the 572 nm band is complete in ~3 min under these conditions and requires neither light nor air. A fairly extensive study of the effect of temperature and pH on the conversion of rC_{552} to p572 revealed the following. At pH 7.2 and 70 °C, the conversion is first-order over several half-times of the reaction; $k_{obs} \sim 30\ s^{-1}$. The conversion fraction, moles of p572 per initial moles of rC_{552}, is ~0.3 and is independent of temperature. The activation energy (E_a) for this reaction is ~25 kcal/mol, accounting for the slowness of the reaction at cold-room temperatures. The ratio of p572 to starting rC_{552} is strongly pH dependent, being zero at pH 6, ~0.3 at pH 8.3, a maximum of ~0.5 at pH 10, and zero at pH 13. Thus, a higher pH favors rC_{552}-to-p572 conversion, suggesting the possible involvement of a catalytic base.

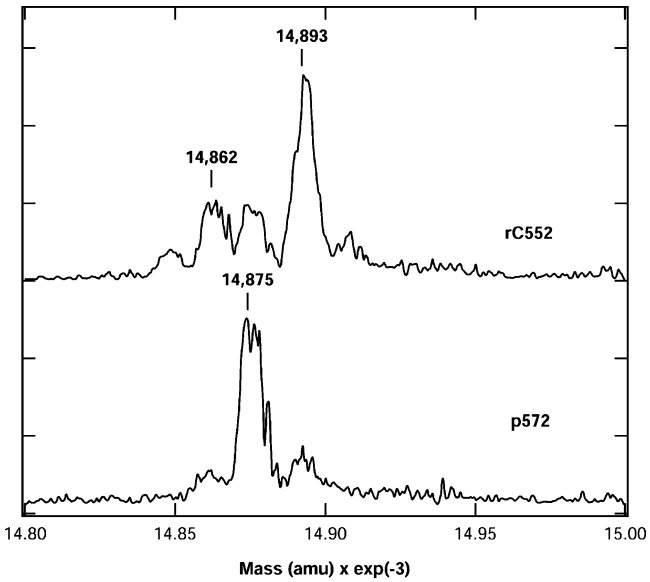

FIGURE 2: Electrospray mass spectra of recombinant cytochrome rC_{552} and p572 dissolved in 10 mM ammonium acetate and freed from Na^+ ions by gel filtration. Cytochrome rC_{552} exhibits peaks at 14 862, 14 875, and 14 893 Da, while p572 exhibits a very weak signal at 14 862 Da, a dominant signal at 14 875 Da, and a very weak signal at 14 893 Da. Spectra were recorded as described in Experimental Procedures.

qualitative observations that treatment with excess hydrazine, borohydride, or cyanoborohydride (see ref *39* and references therein) shifted the 572 nm absorption band to ~550 nm (data not shown).

Mass Spectrometry

Mass spectral studies provided the first clue to the origin of the new chromophore. Figure 2 shows electrospray mass spectra of rC_{552} (top) and purified p572 (bottom). The expected mass of the recombinant rC_{552} is 14 862 Da (*11*). Instead, we observe three components as described previously (*11*). The top spectrum shows a dominant peak at 14 893 Da, a second, weaker peak at 14 875 Da, and, at similar intensity, the expected peak at 14 862 Da. (The origin of the smallest peak, at ~14 848 Da, is not known.) p572 shows a major peak at 14 875 Da, corresponding to the central peak observed with rC_{552}, and minor peaks at 14 862 and 14 893 Da. Given that the uncertainties in the experimental masses are approximately ±2 Da, the dominant feature of rC_{552} is the presence of an unexpected, additional mass of (14 893 Da *minus* the constant 14 862 Da) ~31 ± 2 Da. Similarly, p572 contains an additional (14 875 Da *minus* 14 862 Da) ~13 ± 2 Da. These data are broadly consistent with the presence of two additional O atoms in rC_{552} and one additional O atom in p572, not considering loss of protons (see below).

The availability of relatively small amounts of rC_{552} (*15*) and even smaller amounts of p572 obviated large-scale isolation and heme extraction from the protein, as has been done with other cytochromes *c* (see refs *40* and *41*, for example). Therefore, to further characterize the modified heme, we degraded holoprotein with pepsin followed by high-resolution mass spectrometry of chromatographically purified, heme-containing peptides (see Experimental Procedures). The heme peptide prepared from rsC_{552} is expected to have the amino acid sequence Ala-Gln-Cys-Ala-Gly-Cys-His-Gln-Gln-Asn-Gly-Gln-Gly-Ile-Pro-Gly-Ala-Phe with the heme attached to the two cysteine residues via thioether links. The monoisotopic mass of the singly protonated form of this entity is 2402.96 Da, while the isotopically averaged mass is 2404.49 Da. Additional data are presented in the Supporting Information (Table 1-SM) and lie within the error limits of these predicted values, thus confirming its structure. By contrast, heme peptide isolated from p572 by the same procedure and subjected to identical treatment shows masses 12−13 Da greater[3] (Table 1-SM). The mass spectral data thus impose an important boundary condition on the possible chemistry by which rC_{552} converts to p572, namely, that there can be no further addition of, e.g., O atoms (see Discussion).

Table 2: Optical Absorption Properties of the Cytochromes Used in This Study

peak	Soret (nm)	β (nm)	α (nm)
native c_{552}	409		
oxidized	417		
reduced		525	552
reduced			21100[a]
reduced minus oxidized			14300[a]
rC_{552}			
oxidized	410		
reduced	417	522	552
reduced minus oxidized			12200[a]
p572			
oxidized	416		
reduced	430	537	572
reduced			22400[a]
reduced minus oxidized			13200[a]

[a] ϵ, $\Delta\epsilon$ (M^{-1} cm^{-1}).

Crystallographic Characterization of rC_{552}

Crystals of rC_{552} were grown at 4 °C to minimize conversion to p572 (see Experimental Procedures), mounted on nylon loops, flash-frozen, and transported to SSRL at liquid nitrogen temperature. After data collection at 100 K, one crystal was dissolved into a minimum volume of buffer at ice temperature. The optical absorption spectrum of the dissolved protein registered the complete absence of either 552 or 572 nm bands, indicating no significant reduction or conversion of heme had occurred while in the X-ray beam. Once this solution had been heated for a few moments, a strong band appeared at 572 nm, indicating that factors vital to the conversion of rC_{552} to p572 were retained during the crystallographic experiment (not shown).

The structure of rC_{552} was determined at a resolution of 1.41 Å (Table 1), and coordinates and structure factors have been deposited with the Protein Data Bank (entry 1QYZ). The overall structure is generally similar to that of native cytochrome c_{552} (PDB entry 1C52) or native-like, recombinant rsC_{552} (PDB entry 1DT1); see Figure 3A. Differences between the structures of native c_{552} and p572 exist in the lysine rich region from Lys95 to Lys101, where the electron density map of the latter does not permit the main chain to be traced. Similar disorder was reported for the native-like rsC_{552} structure (*21*), and in the rC_{552} structure, the chain could not be traced from Val97 through Gly99. These

[3] We have not attempted to isolate a heme peptide from rC_{552} because of the likelihood that it would spontaneously convert to p572 during the experiment.

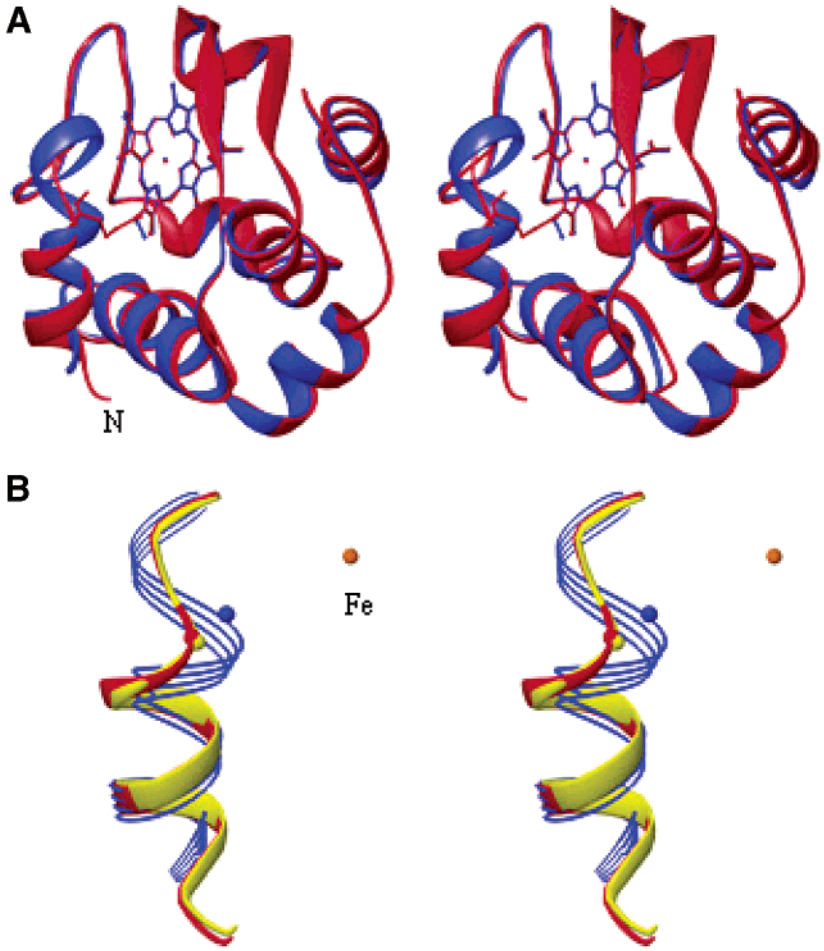

FIGURE 3: Stereoview (wall-eye) showing overlapping structures of native rC_{552} and p572. (A) The complete native (rsC_{552}) structure is shown as a blue ribbon overlapped with that of rC_{552} as a red ribbon. Proteins were aligned on the basis of their heme positions. This structure contains the heme-to-cysteine 11 bridge as a ball-and-stick model. Significant differences between the protein structures are seen only in the region of residues 10−13. (B) Overlapping ribbon structures (N-terminus to Cys14) of rsC_{552} (red), rC_{552} (blue), and p572 (yellow). The small colored balls correspond to the positions of the cytsteine 11 C_α atom in each structure. The program RIBBONS recognizes residues 11−15 in rC_{552} and residues 9−15 in p572 as β-turn and coil rather than α-helix as in rsC_{552}. The Fe-to-cysteine 11 C_α distances are 6.51 Å for rsC_{552}, 8.92 Å for rC_{552}, and 8.92 Å for p572.

differences were previously attributed to differences in intermolecular packing in the different crystal types rather than real differences in structure and are not discussed further. It is also noteworthy that the heme and the axial ligand positions do not differ significantly from those in the native structure.

There are significant structural differences in the region of heme ring I and nearby residues, Gln10, Cys11, Ala12, and Gly13, within which Cys11 lies ~3 Å farther from the heme than in the native structure (see Figure 3B). On either side of this stretch of the polypeptide, the structure of the protein is highly similar to that of the native protein. Particularly important is the normal thioether linkage between Cys14 and the 4-vinyl group of heme ring II and coordination of the His15 Nδ and Met69 Sγ atoms to the heme iron. By contrast, the electron density shows an abnormal thioether linkage among ring I, 2-vinyl, and Cys-11. This is evident in the experimental electron density (as an "omit" map in which Cys11 is replaced by Gly at position 11) of this region (see Figure 4), and the model is consistent with a CO-CH_2-S-CH_2 bridge between the heme and cysteine 11. Here we have superimposed an $|F_o| - |F_c|$ map on an atomic model that accounts for the experimental structure factors; the metric features of the bridge are summarized in footnote 4. Efforts to fit the observed electron density with that expected from a C_A peroxide adduct (*42*) were unsuccessful because the hydrophobic side chain of Phe72 occupies the only space available for the second O atom of a peroxide. It is possible that the Phe72 side chain is not properly folded against the heme during the collapse of the protein about the heme.

A search of the literature revealed that this arrangement of atoms has been found previously in nature as ethylthiopropan-2-one (*43*) and has been synthesized on a few occasions (refs *44*−*46* and references therein), although little is known about its chemical reactivity. Assembled within a steroid-like compound, an X-ray structure has been determined (*46*; Cambridge Crystallographic Structure Database

[4] The electron density map of rC_{552} shows no evidence of a partial occupancy from native-like material in which a normal C_A thioether linkage occurs at 2-vinyl. Metric features of the bridge: heme 2−C_A distance = 1.44 Å, C_A−O distance = 1.44 Å, C_A−C_B distance = 1.61 Å, C_B−S_γ of cysteine 11 distance = 2.12 Å, S_γ−C_β of cysteine 11 distance = 1.82 Å, and C_β−C_α distance = 1.53 Å (approximate errors of ±0.05 Å). The angles starting from heme 2 are as follows: 119.2° for heme 2−C_A−CB, 93.1° for C_A−C_B−S_γ, 123.2° for C_B−S_γ−C_β, and 115.4° for S_γ−C_β−C_α. The torsion angles starting from heme 2 are as follows: −172.1° for heme 2−C_A−C_B−S_γ, 64.6° for C_A−C_B−S_γ−C_β, and 87.6° for C_B−S_γ−C_β−C_α. Approximate errors in angles are ±2°.

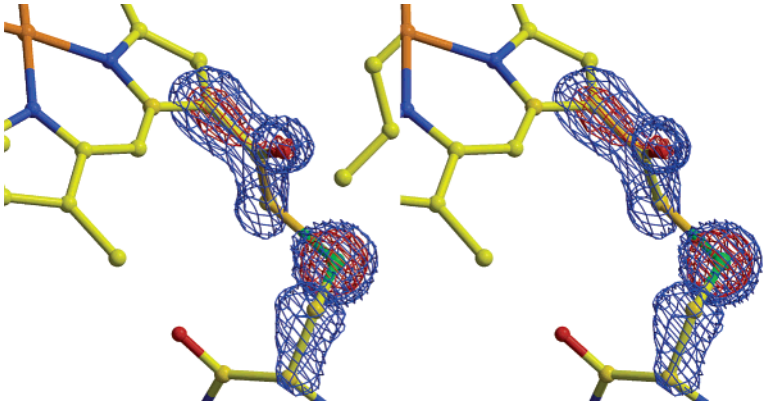

FIGURE 4: Stereoview (wall-eye) of an omit map ($|F_o| - |F_c|$) of the Cys11−heme ring I region in rC_{552}, including a model derived from Scheme 1. Heme atom C3B, 2-vinyl atoms C_A and C_B, and cysteine 11 atoms Sγ, C$_\beta$, and C$_\alpha$ were omitted from the electron density calculation. The model corresponds to the proposed CO-CH_2-S-CH_2-C$_\alpha$ structure made up of the original 2-vinyl atoms and those of cysteine 11. Contour levels: blue for 3σ and red for 5σ.

reference number 177055), which is quite similar to that reported above except for a significantly different $C_B-S_\gamma-C_\beta-C_\alpha$ torsional angle (−117.96° vs +87.6°).[5]

The proposed bridging structure would not, at first sight, be expected to be very reactive. Indeed, this arrangement of atoms is apparently stable at room temperature in water and in brine, as noted (*46*). However, within rC_{552}, it appears to be quite reactive and can be converted to p572, as noted above.

To account for formation of the bridge, we suggest that the S_γ atom of Cys11, as either a thiolate or a thiyl radical, reacts with C_B of the 2-vinyl group with subsequent reactions involving O_2 yielding a C_A−peroxo intermediate which decays to the bridge structure observed in the crystal. See Scheme 1 in the Discussion.

Crystallographic Characterization of p572

Crystals of p572, isomorphous with those of rC_{552}, were grown at room temperature and diffracted to 1.61 Å (PDB entry 1ROQ) (Table 1). The general structure is very similar to that of native (1C52) and native-like, recombinant rsC_{552} (1DT1). In this case, the crystal was not examined for one-electron reduction in the X-ray beam.

As in the case of rC_{552}, outside of the amino acid sequence region of residues 10−13, there are no significant differences between p572 and the native cytochrome *c* structure. As with rC_{552}, p572 contains a normal thioether linkage between Cys14 and the 4-vinyl group of heme ring II. However, important differences, relevant to the distinguishing properties of p572, occur at the 2-vinyl on heme ring I and in the region of Gln10, Cys11, Ala12, and Gly13 compared with both native and rC_{552} structures. Indeed, the polypeptide chain in this region is very similar to that of rC_{552} (see Figure 3B). Figure 5A shows an "omit" ($|F_o - F_c|$) map of the space about heme ring I and Cys11. A carbonyl group accounts for the portion of the difference map near the heme, likely formyl, lying approximately within the plane of the porphyrin (Figure 5B); there appears to be a weak connection between 2-vinyl C_A and Cys11 in p572, suggesting some heterogeneity in the p572 reaction product. The electron density map in the region of cysteine 11 is dominated by two large peaks evidently due to disorder of the cysteine 11 S_γ atom. A single round of refinement of the structure using REFMAC5, as part of the CCP4 suite of programs (*27*), suggested the two peaks could be modeled with relative *S* occupancy of ∼0.65 and ∼0.35. This accounts for the large peaks of density but leaves some 4σ positive difference density near the smaller of the two *S* peaks (not shown). Thus, we were unable to model the difference data satisfactorily with two conformations of Cys11 using normal torsion angles. This residual error may reflect the presence of the putative thiirane CH_2 atoms, although it is not sufficiently defined to attempt a fit using an *R*/*S* mixture of cysteine 11 thiiranes (see below). The Gln10, Cys11, Ala12 region is not well fit by the current model, perhaps because of structural heterogeneity. For these reasons, it is important not to overinterpret the observed electron density in this region (see the Discussion).

Spectral Characterization of rC_{552} and p572

The spectral properties of these aberrant cytochromes *c* should support the proposed crystallographic structures. Accordingly, we have examined rC_{552} and p572 by UV−visible optical absorption, circular dichroism, rR, and high-frequency ^{1}H NMR spectroscopies.

Optical Absorption Spectra. Spectra shown in Figure 1 that arise from the low-spin, Fe(II) versions of the particular cytochromes *c* are generally known to arise from $\pi-\pi^*$ transitions of the porphyrin macrocycle. Details, including wavelength and intensities, of these transitions are influenced by, and therefore carry information about, porphyrin side chains, the nature of the ligands on the heme iron, and the environment within the protein (cf. refs *32* and *47*−*50*). For example, in native and native-like cytochromes c_{552} and rsC_{552}, respectively, the $\mathbf{Q_{00}}$ transition is split into two transitions resulting from perturbations that lower the normally D_{2h} symmetry of the porphyrin and lead the normally degenerate e_g levels to assume different energies (*51*−*53*). Indeed, the similarity of spectral splitting in these proteins indicates their structural identity (*21*). A strong indication that rC_{552} is structurally different from the native-

[5] The analogous distances in (*S*)-6α,9α-difluoro-11β-hydroxy-16α,17α-isopropylidenedioxy-21-(2-oxotetrahydrofuran-3-ylsulfanyl)-pregna-1,4-diene-3,20-dione (*46*) are as follows: 1.53 Å for $C_{17}-C_{20}$, 1.23 Å for $C_{20}-O_5$, 1.46 Å for $C_{20}-C_{21}$, 1.79 Å for $C_{21}-S_1$, 1.79 Å for S_1-C_{22}, and 1.52 Å for $C_{22}-C_{25}$. The corresponding angles are as follows: 118.53° for $C_{17}-C_{20}-C_{21}$, 118.24° for $C_{21}-C_{21}-S_1$, 103.43° for $C_{21}-S_1-C_{22}$, and 109.62° for $S_1-C_{22}-C_{25}$. The corresponding torsional angles are as follows: −166.75° for $C_{17}-C_{20}-C_{21}-S_1$, −70.00° for $C_{21}-C_{21}-S_1-C_{22}$, and −171.96° for $C_{21}-S_1-C_{22}-C_{25}$.

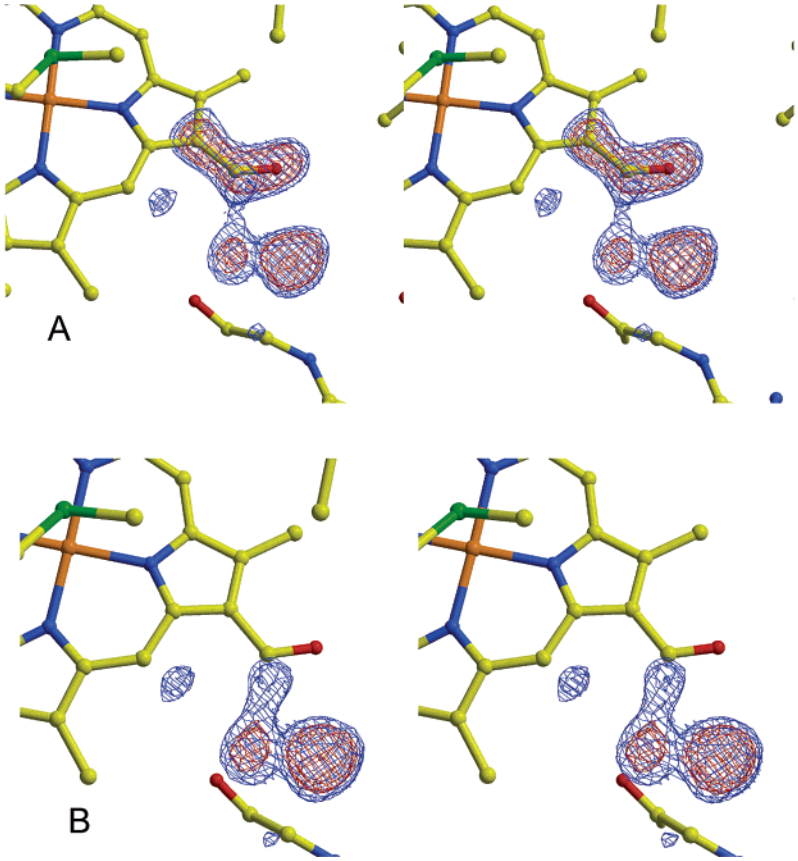

FIGURE 5: (A) Stereoview (wall-eye) of an omit electron density map ($|F_o| - |F_c|$) of the Cys11−heme ring I region of p572 obtained by omitting atoms C3B, CAB, and OAB from the heme model and converting Cys11 to a glycine residue. (B) Similar omit map obtained by including the above heme atoms in the refinement while retaining glycine in place of cysteine at position 11. While showing convincing evidence for the 2-formyl group, three weak to strong peaks of electron density remain unexplained (see the text). Contour levels: blue for 3σ and red for 5σ.

like protein is the apparent absence of $\mathbf{Q_{00}}$ splitting in rC_{552} (see Figure 8 of ref *11*).

The dramatically shifted γ and $\mathbf{Q_{00}}$ bands of p572 (see Table 2) indicate a structural change affecting the energy levels of A_{1u}, A_{2u}, and possibly e_g. It is well-known that electrophilic side chains such as vinyl and formyl cause the visible and Soret bands to shift to longer wavelengths (*54*, *55*). The pyridine hemochromogen spectrum of p572 has a peak at ~581 nm, which is essentially identical with that of 2(4)-formyldeutero IX porphyrin (*32*) and slightly lower in energy than that of heme A[6] (*24*). This provides rather strong evidence for the presence of a monoformyl porphyrin that, because of the Cys14−4-vinyl thioether link, also does not have a vinyl group. Note that optical spectra would likely not distinguish the following possible bridging structures in rC_{552}: (a) the C═O group is orthogonal to the plane of the heme, (b) the C_A had reacted with a hydrogen atom as opposed to O_2 to form CH_2 at C_A (see below), and (c) an sp^3 C_A atom bearing a hydroperoxide group.

CD Spectroscopy. As shown in the Supporting Information (Figure 1SM), the far-UV CD spectrum of rsC_{552} displays minima at 208 and 222 nm, as expected for a protein with a high α-helical content. The spectrum of rC_{552} also has minima at 208 and 222 nm, but with intensities significantly lower than those observed for rsC_{552} (panel A of Figure 1SM). This may reflect the slightly lower α-helical content in rC_{552} that can be seen in the structure (Figure 3A,B). The CD spectrum of rsC_{552} in the Soret region displays a large positive band at 405 nm and a small negative band at 417 nm, whereas the Soret CD spectrum of purified rC_{552} has positive (403 nm) and negative (417 nm) bands with intensities similar to each other (panel B of Figure 1SM). The positive Soret CD band of rC_{552} is significantly lower in intensity (by a factor of 2) than that for rsC_{552}. The CD spectrum in this region arises from protein-induced deformation of the heme (*56*) and from the interaction of the heme with aromatic groups in its vicinity (*57*). Although small, these shifts nevertheless demonstrate that the local heme environment in rC_{552} is significantly perturbed. The lower intensities in rC_{552} may indicate the presence of substantial structural heterogeneity in the molecule, or as suggested by Wittung-Stafshede (*58*), newly isolated rC_{552} may have the properties of a "molten globule".

Raman Spectroscopy. Resonance Raman (rR) spectra (*59*) have been reported for native cytochrome c_{552} (*60*, *61*) and native-like, recombinant rsC_{552} (*21*). We present spectra of oxidized and reduced forms of cytochromes rsC_{552}, rC_{552}, and p572. Table 3 summarizes the normal-mode frequencies (*62*) that we have assigned. Primary spectra are shown in Figure 6 and Figures 2SM−5SM of the Supporting Information.

The data for the recombinant rsC_{552} are indistinguishable from those of native cytochrome c_{552} published previously

[6] Note that heme A, which has one formyl and vinyl group each, has its pyridine hemochrome maximum at ~586 nm (*24*).

Table 3: Resonance Raman, Normal-Mode Frequencies (cm^{-1}) of *T. thermophilus* Recombinant Cytochromes rsC_{552}, rC_{552}, and p572

	oxidized[a]			reduced[a]		
normal mode	rsC_{552}	rC_{552}	p572	rsC_{552}	rC_{552}	p572
$\nu_{C=O}$	none	none	1666	none	(1643[d])	1645
ν_{10}	1633[a]	1632 (1636[b])	1633 (1635[b])	1622	1622 (1622[b])	1621 (1623[b])
ν_{38}	–	–	–	1606	1606	1606
ν_2	1584	1584	1576	1588	1585	1579
ν_{19}	nr[c]	1586[b]	1585[b]	nr[c]	1586[b]	1587[b]
ν_{11}	1557(?)	~1560	–	1541	1557	~1560
		1558[b]	1554[b]		1541[b]/1558[b]	1553[b]
$2\nu_{15}$(?)[e]	–	–	–	nr[c]	1518[b]	1513[b]
ν_3	1503	1503	1500	1491	1491	1490
ν_4	1371	1371	1370	1359	1359	1358
ν_{13}	1236	1235	nr[c]	1228	1228	nr[c]
ν_{15}	747	746	nr[c]	749	747	nr[c]
νC_A-S[f]	691	688	nr[c]	689	685	nr[c]
$\delta C_\beta C_A C_B$	412	418	nr[c]	414	weak	nr[c]
γ_{22}	440	–	nr[c]	440	–	nr[c]
$\delta C_\beta C_C C_D$ (propanoate)	377	377	nr[c]	378	377	nr[c]
ν_8	345	346	nr[c]	345	346/354 (?)	nr[c]

[a] Unless noted otherwise, the excitation wavelength was 413 nm. [b] Excitation wavelength of 568 nm. [c] Not recorded. [d] Arises from contaminating p572. [e] Assignment uncertain. Hu *et al.* (*63*) assign a similar feature in the spectra of yeast cytochrome *c* to this overtone, but the frequency we observe here is not double the ν_{15} frequency. [f] Assignment for yeast protein and rsC_{552} (*63*). The normal mode necessarily changes in the modified linkage of rC_{552}.

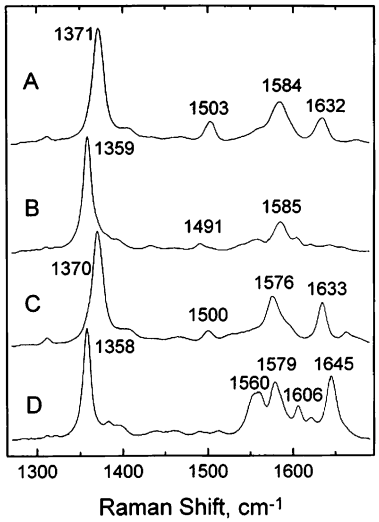

FIGURE 6: Resonance Raman spectra of *T. thermophilus* recombinant cytochrome rC_{552} and p572 in the high-frequency region obtained with Soret band excitation at 413 nm at room temperature: (A) oxidized rC_{552}, (B) reduced rC_{552}, (C) oxidized p572, and (D) reduced p572. The typical sample concentration is 20−30 μM, with a 2400 groove/mm grating; the entrance slit was set to 150 μm, and data were accumulated over a period of 5 min. All spectra were recorded at room temperature, and the typical sample concentration was 20−30 μM in 100 mM Tris-HCl buffer (pH 8). Additional spectra are provided in the Supporting Information.

(*21*, *60*) (see Figures 2SM and 3SM, dotted lines). Moreover, these spectra are also very similar to those of yeast cytochrome *c* (*63*). The comparison is obvious for the spectra of oxidized adducts all recorded at room temperature. However, the spectra of reduced yeast cytochrome *c* in the study by Hu *et al.* (*63*) were recorded at 12 K, affording greater resolution and frequencies ~4−9 cm^{-1} higher than those obtained at room temperature. Given this, the rR spectra of ferrocytochrome rsC_{552} and yeast ferrocytochrome *c* are quite similar, confirming the similar chromophores and immediate protein environment in these homologous proteins.

As shown in Table 3, normal-mode frequencies (*62*) ν_{10}, ν_{19} (observed with visible excitation), and, to a lesser extent, ν_3 are essentially unchanged for rsC_{552}, rC_{552}, and p572, confirming identical spin and coordination states of the central Fe in both oxidation states of all three cytochromes. Also similar are the ν_4 frequencies, which are useful in identifying the Fe oxidation state. On the other hand, frequencies of modes involving the periphery of the porphyrin and its substituents, that is, ν_2 and ν_{11}, show differences ranging from 8 to 20 cm^{-1}, consistent with changes in the heme periphery, in both oxidized and reduced adducts, among the three species.

Regardless of oxidation state or excitation wavelength, the rR spectra of rsC_{552} and rC_{552}, compared in Figures 2SM and 3SM of the Supporting Information, are quite similar. This implies that little overlap occurs between the carbonyl group of the bridge and the heme π-electron system in rC_{552}. As noted above, the observed ~70° angle between the carbonyl and heme planes is sufficiently close to orthogonal to prevent conjugation and resonance enhancement of carbonyl vibrations in the rR spectrum of rC_{552} (*64*−*68*). This explains the overall similarity to that of spectra of rC_{552} and rsC_{552}, despite their significant structural differences.

Our spectra confirm identical axial ligation in all three adducts but demonstrate differences in the peripheral substituents. The low-frequency feature at 412 cm^{-1} in the spectrum of oxidized rsC_{552} increases in frequency to 418 cm^{-1} and decreases in intensity in the spectrum of oxidized rC_{552} (Figure 3SM of the Supporting Information, trace A). Similar differences are noted in the spectra of the reduced adducts (Figure 3SM, trace B). This feature is assigned to the $C_\beta C_A C_B$ bending motion of the covalent Cys linkages (*63*). The *intensity decrease* is consistent with the crystallographic data. That is, as the C_A═O group is held roughly orthogonal to the heme plane in the rC_{552}, the C_B position and the vibrational bending motion itself are forced out of plane and are no longer resonance-enhanced in the spectrum of rC_{552}. Similarly, the *increased frequency* of the bend is consistent with the greater s character of C_A and, hence,

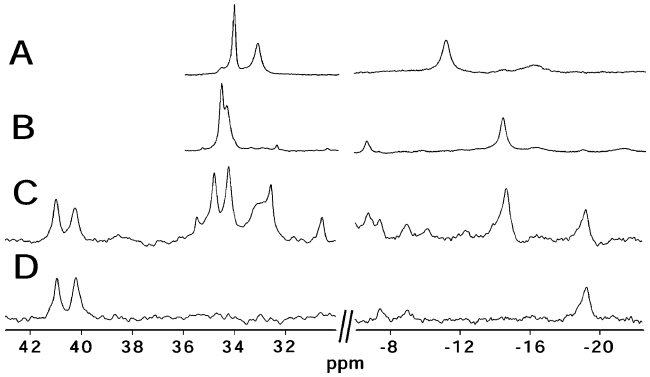

FIGURE 7: ^{1}H NMR spectra at 25 °C for oxidized cytochrome rsC_{552} (A) and cytochrome rC_{552} as isolated (B), after heating the latter to 70 °C for 30 min followed by cooling to 25 °C and oxidation with ferricyanide (C) and p572 (D). Sample D was purified from sample C. See Experimental Procedures for details of the recording.

strengthened C−C bonds in the ring I−cysteine 11 linkage of rC_{552} compared to rsC_{552}. On the other hand, the weaker feature at ~377 cm^{-1}, attributed to a bending motion of the propionate groups, remains unchanged in all spectra, reflecting the fact that the structural variations in the heme periphery are confined to the covalent linkages with the protein.

The high-frequency rR spectra of oxidized and reduced rC_{552} (Figure 6, traces A and B, respectively) and oxidized and reduced p572 (Figure 6, traces C and D, respectively), all obtained with 413 nm excitation, are shown in Figure 6. The rR spectra of p572 are clearly distinct from those of c_{552} proteins and yeast cytochrome *c*, reflecting the movement of the carbonyl group into the overall heme plane. The strong feature at 1645 cm^{-1} corresponds to a "formyl" stretch, and is known only in A-type hemes (*69*), the *Spirographis* hemes (*70*), and photosynthetic pigments having a formyl substituent (*71*). This feature confirms the presence of a formyl group and provides further support that it is conjugated and therefore coplanar with the porphyrin ring (*64*−*68*). Likewise, a weaker feature at approximately 1666 cm^{-1} in the spectrum of oxidized p572 is also assigned to the formyl C═O stretching mode (Figure 6, trace C, not labeled). Both the frequency decrease and intensity increase upon reduction are readily interpretable and consistent with those observed for the a_3 formyl groups of cytochromes aa_3 (*69*, *72*) and ba_3 (*73*). Indeed, the frequency of the strong 1645 cm^{-1} feature is low relative that of analogous A-type cytochromes (57), consistent with its position on the heme. Indeed, Tsubaki *et al*. (*70*) demonstrated that this frequency is sensitive to the formyl position on asymmetrically substituted hemes and that a formyl substituent on the C2 position of a ferrous myoglobin derivative resulted in a frequency of 1648 cm^{-1} compared to the frequency of 1660 cm^{-1} observed from a C4 formylated derivative. Thus, the 1645 cm^{-1} frequency is evidence of a conjugated formyl group on C2 of ring I, as supported by the crystallographic results.

NMR Spectroscopy. Paramagnetically shifted heme methyl resonances reveal important details of electron spin delocalization on the porphyrin ring (*74*, *75*). The 500 MHz ^{1}H NMR spectra of cytochrome rsC_{552} and of cytochrome rC_{552} before and after heating, with a particular emphasis on the hyperfine-shifted resonances of the heme, are shown in Figure 7A−C. The well-resolved resonances at 34.8 and 34.2 ppm (shifts from spectrum in Figure 7B) in the spectrum of oxidized, unheated rC_{552} have been assigned to heme methyls 3 and 8, respectively, and the upfield-shifted resonance at −15 ppm is assigned to the axial Met ϵ-CH_3 (*16*). After the sample had been heated to 70 °C followed by cooling to 25 °C, and oxidation of the reduced p572 with a small excess of ferricyanide, resonances attributed to p572 appear at 41.0, 40.3, and −19 ppm. The ^{1}H NMR spectrum shown in Figure 7D is that of the oxidized form of purified p572, thereby confirming the assignment described above. The heme methyl resonances in the rC_{552} remaining after heating shift slightly from their positions in unheated rC_{552}, suggesting that the cytochrome molecules that retain $\mathbf{Q_{00}}$ near 550 nm are also modified during heating. We have not further pursued this observation.

The ^{1}H NMR spectrum of oxidized p572 is unique for a cytochrome *c* with His−Met axial ligation, indicating an unusual electronic structure. One novel feature is that it has anomalously large shifts for the two most downfield-shifted resonances (40.3 and 41.0 ppm at 25 °C); typically, the largest shift is ~35 ppm at this temperature for cytochromes *c* with His and Met axial ligands oriented as in p572 (*74*, *76*) (Figure 7). Another unusual property of the p572 NMR spectrum is an unusually large spread of heme methyl resonances [> 30 ppm; compare to 20.5 ppm for rC_{552}, a value typical of cytochromes *c* (*76*)]. The characteristics of the spectrum of oxidized p572 suggest that the electronic structure of the heme has been substantially altered relative to that of rC_{552} or rsC_{552}, each of which has general features typical of cytochromes *c*. As the orientations of the axial ligands are conserved among these species, the unusual heme methyl shift pattern of p572 is attributed to the presence of a formyl group on the macrocycle.

Electron Transfer to Cytochrome ba_3. Finally, a formyl cytochrome *c* is expected to have significantly different electrochemical and electron transferring properties. Cytochrome c_{552} is the natural redox partner of cytochrome ba_3 oxidase in *Thermus* cells grown under microaerophilic conditions (*25*, *77*). As measured under standard assay conditions (*11*), the relative activities of cytochromes rsC_{552}, rC_{552}, and p572 toward *Thermus* cytochrome ba_3 are 1, 0.85, and ≤0.1, respectively. Because it is difficult to eliminate rC_{552} from preparations of p572, the latter number represents an upper limit, and we suspect the activity with p572 is considerably lower.

Electrochemistry

Preliminary, reductive titrations of heated, as-isolated rC_{552} with ascorbate revealed that the 572 nm peak preceded the appearance of the 552 nm peak, suggesting that p572 may have a higher reduction potential than the remaining cytochrome *c*. Accordingly, we measured the reduction potential of purified p572 (trace A in Figure 6SM), an ~80:20 mixture of rC_{552} and p572 (trace B in Figure 6SM), and native-like rsC_{552} (trace C in Figure 6SM) using cyclic voltammetry. The midpoint potentials (E_m) derived from these voltammograms are 200 mV for rsC_{552} and 340 mV for p572 (vs the standard hydrogen electrode). As determined from the reduced minus oxidized optical absorption spectrum, the rC_{552} sample used in this experiment was an ~80:20 mixture of rC_{552} and p572 accounting for the much broader cyclic

voltammogram and the shoulder at ~325 mV (trace B in Figure 6SM); the midpoint potential of rC_{552} is estimated to be ~220 mV, approximately 20 mV higher than that of rsC_{552}. The large positive shift in reduction potential seen for p572 is consistent with the expected effects on heme reduction potentials of carbonyl or Schiff base coupling into the porphyrin π-system (*32*). Finally, assuming that steady state oxidase activity may be limited by the transfer of electrons from the cytochrome *c* to the Cu_A site of ba_3 (~240 mV), the very high potential of p572 (~340 mV) accounts for its greatly reduced electron transfer activity with cytochrome ba_3.

DISCUSSION

During synthesis in the cytoplasm of aerobically grown *E. coli*, cytochrome rC_{552} appears to bind two O atoms, thereby retaining in its molecular structure the capacity to spontaneously convert from a chromophore having a $\mathbf{Q_{00}}$ transition at ~550 nm, typical of a heme having no double bonds conjugated to the porphyrin π-system, to a chromophore with a formyl group that is strongly conjugated with the heme π-system (p572), having a $\mathbf{Q_{00}}$ transition at 572 nm. In effect, this conversion results in the oxidation of the 2-vinyl group of iron protoporphyrin IX to [2-formyl-4-vinyl] or *Spirographis* heme (*78*). In the course of this conversion, rC_{552} decreases its mass by ~13 ± 4 Da. This occurs by a novel mechanism involving O_2 and the Cys11 residue[7,8] and, by comparison to organic routes, does not involve the use of powerful and somewhat indiscriminate oxidants.[9]

A substantial body of data on the spectral, mass, and structural properties of rC_{552} and p572 supports the chemistry suggested below in Schemes 1 and 2. These data show unequivocally and without exception that (a) Cys11, the heme 2-vinyl group (on heme ring I; cf. ref *32*), and presumably O_2[8] are the primary players in an unusual chemistry, (b) a bridge of electron density in rC_{552} maps extends from the 2-position of the heme to the C_α atom of cysteine 11 which corresponds to the presence of $CO\text{-}CH_2\text{-}S\text{-}CH_2$ atoms, (c) the plane of CO in this bridging group is approximately normal to the plane of the heme, (d) the vinyl $C_A{-}C_B$ bond is broken in p572 and C_A is oxidized to a formyl group, and (e) only one extra O atom resides in the final p572 product, presumably in the formyl group.

To account for the formation of the heme-to-protein bridge in rC_{552}, we suggest the chemistry shown in Scheme 1. This originates in a reaction of the Cys11 S_γ atom [either as a thiolate (top) or as a thiyl radical (bottom)] with the C_B atom ($=CH_2$) of 2-vinyl. In both paths, this is followed by

Scheme 1

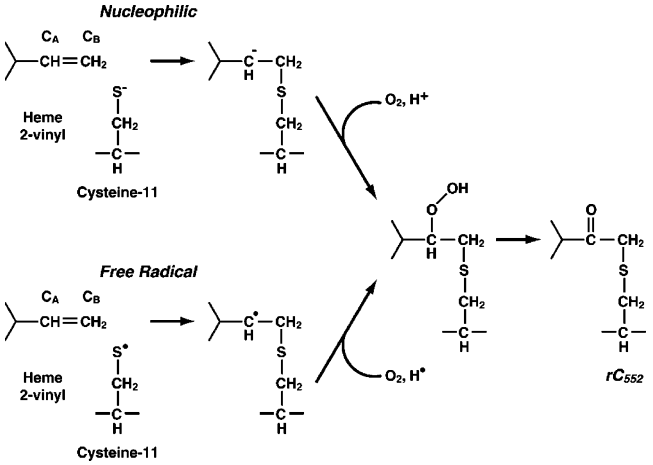

reaction of O_2 with the resulting carbanion or free radical at C_A which ultimately forms a hydroperoxide moeity. The anti-Markovnikov addition of RS to the 2-vinyl would generally suggest a free radical route (*79*), where the cysteine radical may result from spurious oxidation. However, a thiolate is also possible because improper folding of the N-terminal region against the main body of the protein may hold the S_γ of Cys11 away from C_A, and stabilization of a carbanion on C_A through conjugation with the porphyrin π-system could facilitate nucleophilic attack of $RS\gamma^-$ at C_B of the 2-vinyl, consistent with the pH dependence of the reaction.[2] Similarly, a free radical at C_A may be stabilized in its sp^2 configuration, thereby facilitating reaction with O_2. Subsequent dehydration of the hydroperoxide to the carbonyl corresponds to a four-electron oxidation of the vinyl group.[10] Lightner *et al.* (*80*) have noted both Markovnikov and anti-Markovnikov adducts in both photochemical and acid-catalyzed thiol addition to one of the vinyl groups of bilirubin.

Scheme 2

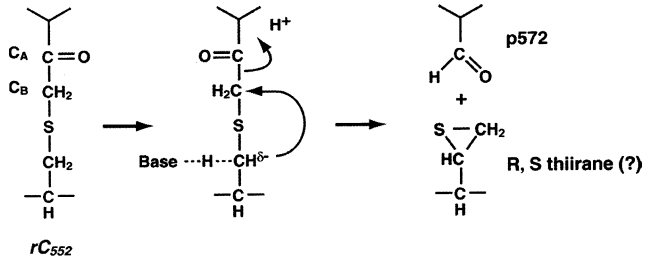

The rather speculative Scheme 2 is offered, which leads to a product consistent with the observed molecular masses, crystal structure, and spectral properties of p572. Here, the abnormal thioether loses a proton in a base-assisted process,[2] forming an incipient carbanion on the C_β atom of cysteine 11 which, as the simplest means of cleaving the $C_A{-}C_B$ bond of the original 2-vinyl group, we suggest, attacks the C_B carbon of the erstwhile 2-vinyl group, with attendant formation of a thiirane at cysteine 11 (see refs *81* and *82* for

[7] Recently, evidence that thiolate groups can exhibit novel chemical behavior when associated with proteins has accrued, for example, unexpected disulfide formation (*16*), oxidation to sulfenates and sulfonates (*83*), involvement in the oxidation of porphyrin side chains (*84*), and formation of a cyclic sulfenyl amide (*85*). We add to this list a protein−thiol-mediated oxidation of a heme vinyl to a heme formyl substituent.

[8] *E. coli* cells able to synthesize rC_{552} when grown aerobically fail to produce any cytochrome c_{552} when grown anaerobically. We therefore assume that the presence of 31 ± 2 Da in the mass of rC_{552}, obtained from aerobically grown cells, indicates the presence of two additional O atoms in the as-isolated form of this protein.

[9] There are several synthetic methods for the oxidation of a ring-bound vinyl group to a formyl group: $KMnO_4$ and OsO_4 (*39*), OsO_4/$NaIO_4$ (*86*), singlet oxygen (*87*), and ozonolysis (*88*).

[10] Formally, the valence of C in methane is −IV, 0 in diamond, and +IV in CO_2, and the valence of the cysteine 11 S_γ atom is maintained at (−II). If only internal oxidation and reduction occur upon conversion of rC_{552} to p572, C_A is reduced from C(+II) to C(+I) in the formyl while C_β of Cys11 is oxidized from C(−I) to C(0) in the proposed thiirane (Scheme 2).

some discussion of the properties of these compounds) and a formyl group at the original C_A atom. It is reasonable to further suggest that the driving force for this process is the coupling of the π-system of the porphyrin and the formyl group.

Evidence for Scheme 1. The optical and rR spectra suggest that there are no unsaturated side chains in conjugation with the porphyrin macrocycle of rC_{552}. Thus, the $\mathbf{Q_{00}}$ transition is typical of cytochromes *c*, and the rR spectra indicate the core of the heme, particularly those modes composed primarily of porphyrin C−C and C−N vibrations, is highly similar in rC_{552} and native-like rsC_{552}. However, the CD spectra indicate a perturbed heme environment, while the ^{1}H NMR spectra show clearly that the distribution of electron spin density on the porphyrin ring differs in rC_{552} and rsC_{552}. The symmetry of the electronic spin distribution on the porphyrin is also clearly different between these two proteins as evidenced by the changed pattern of methyl resonances (Figure 7, traces A and B). Unfortunately, it is difficult to sort out the underlying structural differences between rC_{552} and native-like rsC_{552} from such spectra.

The crystallographic results, however, indicate a structure that is consistent with the spectral observations. The electron density maps of rC_{552} at a resolution of 1.41 Å show clear bridging density from heme ring I to the C_α atom of cysteine 11, and fixes the angle between the C_A carbonyl plane and the heme plane at ~70°. This seems to preclude significant coupling of the carbonyl π-electrons into the heme π-electron system and makes the bridge appear to the heme as a saturated side chain. Hence, the bridge does not affect the energy of the $\mathbf{Q_{00}}$ transition, but its presence alters the CD and ^{1}H NMR spectra. The combined crystallographic and spectral data do not readily admit to other interpretations and therefore provide strong evidence for the bridge as proposed. As for the suggested chemistry, our data do not distinguish a nucleophilic from a free radical mechanism, and both seem plausible.[11]

Scheme 1 admits the possibility of a side reaction if the putative carbanion at C_A reacts with a proton. This would yield a product having properties, including its molecular weight, similar to those of native-like cytochrome c_{552} (except for the somewhat different protein structure around the Cys11 position). The occurrence of this reaction may account for the observed partial conversion of rC_{552} to p572,[2] the minor band at 14 862 Da corresponding to the molecular mass expected for the native protein (Figure 2), the unique hyperfine-shifted resonances that occur in heated rC_{552} but are not associated with p572 (Figure 7, trace C), and the possible appearance of electron density bridging the heme 2-position and cysteine 11 in the structure of p572 (Figure 5A).

Other data from rC_{552}, however, suggest the system may be somewhat more complicated. For example, the mass spectrum of as-isolated rC_{552} indicates that two additional O atoms are part of the structure, whereas the crystallographic structure of rC_{552} accounts for only one additional O atom. Can this be rationalized? Among several possibilities, we hypothesize that the structure of rC_{552}, as isolated, contains a hydroperoxide group (Scheme 1) which converts to the carbonyl at some point in the process of structure determination and is trapped in the crystal. This might explain why rC_{552}, spectrally free of p572, always shows a significant amount of the 14 875 Da peak in its electrospray mass spectrum (see Figure 2). Current spectral results would likely not distinguish the presence of a hydroperoxide group from that of an unconjugated carbonyl. However, this idea might be tested by determining the mass of rC_{552} that had been subjected to the crystallographic experiment and then dissolved into buffer; crystals treated in such a manner retain their ability to convert to p572, showing that the final bridging structure, lacking the peroxy group, is still able to convert to p572.

Evidence for Scheme 2. Turning to p572, we assume that the instability of rC_{552} with respect to p572 lies in the heme-to-cysteine 11 bridge. Knowing that a conjugated heme formyl substituent is part of p572 makes it reasonable to suggest a mechanism for the conversion of rC_{552} to p572. Key features of Scheme 2 are breaking of the C_A−C_B bond and formation of the C_A carbonyl group which are strongly supported by the crystal structures. Although this is admittedly not the chemical behavior expected from an isolated molecule of R_1-CO-CH_2-S-CH_2-CHR_2 (where R_1 and R_2 are aliphatic), the reaction we are suggesting occurs within a protein molecule where anisotropic forces are likely to affect chemical reactivity (see below).

While crystallography confirms that the bridge between heme and Cys11 is broken and that an isolated, in-plane formyl group has formed on heme ring I, it does not tell us much about what has happened to Cys11. The electron density map in this region is dominated by two large peaks for which the single cysteine 11 S_γ atom can account, and residual positive density only indicates that additional light atoms are present, which may arise from CH_2 atoms in a mixture of (*R*)- and (*S*)-thiirane.

The mass spectra of p572 and its heme peptide are consistent with one extra O atom (compared to a native structure) and the loss of two to four H atoms. Thus, as measured by MALDI-TOF, the expected average mass ($M_{expected}$) of a thiirane containing p572 heme peptide equals 2418 Da (2404 + 16 − 2), while the observed average mass (M_{obs}) equals 2416 ± 2.4 Da (see Table 1-SM). Although other products may fall within this mass range, whatever happens at cysteine 11 does not involve addition of other atoms. For this reason, we have rationalized M_{obs} in terms of a structure in which the S_γ atom of cysteine 11 has become part of a cysteine 11 thiirane (or its mass equivalent). The appearance of the structurally distinct products would contribute to structural disorder in the region of cysteine 11.

In conclusion, the results extend our knowledge of the chemistry that can occur between heme and the CXXCH motif of apocytochromes *c*. We are hopeful this description of cytochrome p572 may suggest more detailed study of protein-bound, formyl-containing hemes, as might occur if these can be prepared *in vitro* (see refs *13*, *22*, and *23*). Certainly, the spectral features of p572 may be useful in the analysis of mixtures of heterologously expressed cytochromes *c*, particularly when mutant forms are being sought (*17*). Finally, the new heme protein chemistry presented here may provide insight into the need for chaperone-directed heme attachment.

[11] It is noteworthy that Carpena and co-workers (*42*) describe a perhydroxy group bound to the 2-vinyl C_A atom in the catalase-peroxidase from *Burkholderia pseudomallei*.

ACKNOWLEDGMENT

We acknowledge useful discussions with Dr. David Goodin of The Scripps Research Institute (La Jolla, CA) and Dr. Linda Thöny-Meyer of ETH (Zurich, Switzerland). We appreciate the work at The Scripps Center for Mass Spectrometry for providing the mass analyses used in this study. We also thank the staff at the Stanford Synchrotron Radiation Laboratory (SSRL) for their excellent support in the use of the beam lines. This work is based on research conducted at SSRL, which is funded by the Department of Energy, Office of Basic Energy Sciences. SSRL beam lines are supported by the National Institutes of Health, the National Center for Research Resources, the Biomedical Technology Program, and the Department of Energy, Office of Biological and Environmental Research.

SUPPORTING INFORMATION AVAILABLE

Additional mass spectral data, circular dichroism spectra, primary resonance Raman spectra, and cyclic voltammograms. This material is available free of charge via the Internet at http://pubs.acs.org.

REFERENCES

1. Thöny-Meyer, L. (2002) Cytochrome *c* maturation: a complex pathway for a simple task? *Biochem. Soc. Trans. 30*, 633−638.
2. Thony-Meyer, L. (2000) Haem-polypeptide interactions during cytochrome *c* maturation, *Biochim. Biophys. Acta 1459*, 316−324.
3. Kranz, R. G., Lill, R., Goldman, B., Bonnard, G., and Merchant, S. (1998) Molecular mechanisms of cytochrome *c* biogenesis: three distinct systems, *Mol. Microbiol. 29*, 383−396.
4. Page, M. D., Sambongi, Y., and Ferguson, S. J. (1998) Contrasting routes of c-type cytochrome assembly in mitochondria, chloroplasts and bacteria, *Trends Biochem. Sci. 23*, 103−108.
5. McEwan, A. G., Kaplan, S., and Donohue, T. J. (1989) Synthesis of *Rhodobacter sphaeroides* cytochrome *c2* in *Escherichia coli*, *FEMS Microbiol. Lett. 59*, 253−258.
6. von Wachenfeldt, C., and Hederstedt, L. (1990) *Bacillus subtilis* holo-cytochrome *c*-550 can be synthesized in aerobic *Escherichia coli*, *FEBS Lett. 270*, 147−151.
7. Grisshammer, R., Oeckl, C., and Michel, H. (1991) Expression in *Escherichia coli* of *c*-type cytochrome genes from *Rhodopseudomonas viridis*, *Biochim. Biophys. Acta 1088*, 183−190.
8. Sanbongi, Y., Yang, J.-H., Igarashi, Y., and Kodama, T. (1990) Cloning, nucleotide sequence and expression of the cytochrome *c*-552 gene from *Hydrogenobacter thermophilus*, *Eur. J. Biochem. 24*, 7−12.
9. Sinha, N., and Ferguson, S. J. (1998) An *Escherichia coli ccm* (cytochrome *c* maturation) deletion strain substantially expresses *Hydrogenobacter thermophilus* cytochrome c_{552} in the cytoplasm: availability of haem influences cytochrome c_{552} maturation, *FEMS Microbiol. Lett. 161*, 1−6.
10. Pollock, W. B. R., Rosell, F. I., Twitchett, M. B., Dumont, M. E., and Mauk, A. G. (1998) Bacterial expression of a mitochondrial cytochrome *c*. Trimethylation of Lys72 in yeast *iso*-1-cytochrome *c* and the alkaline conformational transformation, *Biochemistry 37*, 6124−6131.
11. Keightley, J. A., Sanders, D., Todaro, T. R., Pastuszyn, A., and Fee, J. A. (1998) Cloning and expression in *Escherichia coli* of the cytochorme c_{552} gene from *Thermus thermophilus*: Evidence for genetic linkage to an ATP-binding cassette protein and initial characterization of the *cycA* gene products, *J. Biol. Chem. 273*, 12006−12016.
12. Karan, E. F., Russell, B. S., and Bren, K. L. (2002) Characterization of *Hydrogenobacter thermophilus* cytochromes c_{552} expressed in the cytoplasm and periplasm of *Escherichia coli*, *J. Biol. Inorg. Chem. 7*, 260−272.
13. Daltrop, O., Smith, K. M., and Ferguson, S. J. (2003) Stereoselective *in vitro* formation of *c*-type cytochrome variants from *Hydrogenobacter thermophilus* containing only a single thioether bond, *J. Biol. Chem. 278*, 24308−24313.
14. Hon-nami, K., and Oshima, T. (1977) Purification and some properties of cytochrome c_{552} from an extreme thermophile, *Thermus thermophilus* HB8, *J. Biochem. 82*, 769−776.
15. Keightley, J. A. (1993) Ph.D. Thesis, University of New Mexico, Albuquerque, NM.
16. McRee, D. E., Williams, P. A., Sridhar, V., Pastuszyn, A., Bren, K. L., Patel, K. M., Chen, Y., Todaro, T. R., Sanders, D., Luna, E., and Fee, J. A. (2001) Recombinant cytochrome rC_{557} obtained from *Escherichia coli* cells expressing a truncated *Thermus thermophilus cycA* gene, *J. Biol. Chem. 276*, 6537−6544.
17. Rumbley, J. N., Hoang, L., and Englander, S. W. (2002) Recombinant equine cytochrome *c* in *Escherichia coli*: High-level expression, characterization, and folding and assembly mutants, *Biochemistry 41*, 13894−13901.
18. Sanders, C., and Lill, H. (2000) Expression of prokaryotic and eukaryotic cytochromes *c* in *Escherichia coli*, *Biochim. Biophys. Acta 1459*, 131−138.
19. Arslan, E., Schulz, H., Zufferey, R., Künzler, P., and Thöny-Meyer, L. (1998) Overproduction of the *Bradyrhizobium japonicum c*-type cytochrome subunits of the cbb_3 oxidase in *Escherichia coli*, *Biochem. Biophys. Res. Commun. 251*, 744−747.
20. Ubbink, M., van Beeumen, J., and Canters, G. W. (1992) Cytochrome c_{550} from *Thiobacillus versutus*: Cloning, expression in *Escherichia coli*, and purification of the heterologous holoprotein, *J. Bacteriol. 174*, 3707−3714.
21. Fee, J. A., Chen, Y., Todaro, T. R., Bren, K. L., Patel, K. M., Hill, M. G., Gomez-Moran, E., Loehr, T. M., Ai, J., Thöny-Meyer, L., Williams, P. A., Stura, E., Sridhar, V., and McRee, D. E. (2000) Integrity of *Thermus thermophilus* cytochrome c_{552} synthesized by *Escherichia coli* cells expressing the host-specific cytochrome *c* maturation genes, ccmABCDEFGH: Biochemical, spectral and structural characterization of the recombinant protein, *Protein Sci. 9*, 2074−2084.
22. Daltrop, O., and Ferguson, S. J. (2003) Cytochrome $_c$ maturation: The *in vitro* reactions of horse heart apocytochrome *c* and *Paracoccus denitrificans* apocytochrome c_{550} with heme, *J. Biol. Chem. 278*, 4404−4409.
23. Allen, J. W. A., Barker, P. D., and Ferguson, S. J. (2003) A cytochrome b_{562} variant with a *c*-type cytochrome C*XX*CH heme-binding motif as a probe of the *Escherichia coli* cytochrome *c* maturation system, *J. Biol. Chem. 278*, 52075−52083.
24. Berry, E. A., and Trumpower, B. L. (1987) Simultaneous determination of hemes A, B and C from pyridine hemochrome spectra, *Anal. Biochem. 161*, 1−15.
25. Keightley, J. A., Zimmermann, B. H., Mather, M. W., Springer, P., Pastuszyn, A., Lawrence, D. M., and Fee, J. A. (1995) Molecular genetic and protein chemical charactertization of the cytochrome ba_3 from *Thermus thermophilus* HB8, *J. Biol. Chem. 270*, 20345−20358.
26. Leslie, A. G. W. (1992), Recent changes to the MOSFLM package for processing film and image plate data, *Joint CCP4 + ESF-EAMCB Newsletter on Protein Crystallography*, No. 26, SERC, Daresbury Laboratory, Warrington, U.K.
27. Leslie, A. W. G. (1994) The CCP4 suite: programs for protein crystallography, *Acta Crystallogr. D50*, 760−763.
28. Than, M. E., Hof, P., Huber, R., Bourenkov, G. P., Bartunik, H. D., Buse, G., and Soulimane, T. (1997) *Thermus thermophilus* cytochrome c_{552}: A new highly thermostable cytochrome-*c* structure obtained by MAD phasing, *J. Mol. Biol. 271*, 629−644.
29. McRee, D. E. (1999) XtalView/Xfit: A versatile protein for manipulating atomic coordinates and electron density, *J. Struct. Biol. 125*, 156−165.
30. Sheldrick, G. M., and Schneider, T. R. (1997) SHELXL: High-Resolution Refinement, *Methods Enzymol. 277b*, 319−343.
31. Sheldrick, G. M. (1996) in *Proceedings of the CCP4 study weekend, January 1996* (Dodson, E., Moore, M., Ralph, A., and Bailey, S., Eds.) Daresbury Laboratory, Warrington, U.K.
32. Falk, J. E. (1964) *Porphyrins and metalloporphyrins*, Elsevier, Amsterdam.
33. Smyth, D. G. (1967) Techniques in enzymatic hydrolysis, *Methods Enzymol. 11*, 214−231.
34. Siuzdak, G. (1996) *Mass Spectrometry for Biotechnology*, Academic Press, New York.
35. Fee, J. A., Malmström, B. G., and Vänngard, T. (1970) The reduction of fungal laccase at high pH, *Biochim. Biophys. Acta 197*, 136−142.

36. Brautigan, D., Ferguson-Miller, S., and Margoliash, E. (1978) Mitochondrial cytochrome *c*: Preparation and activity of native and chemically modified cytochromes *c*, *Methods Enzymol. 53*, 128−164.
37. Takemori, S., and King, T. E. (1965) Effect of alkali and borohydride on cardiac cytochrome oxidase: formation of Schiff base, *J. Biol. Chem. 240*, 504−513.
38. Caughey, W. S., Smythe, G. A., O'Keeffe, D. H., Maskasky, J. E., and Smith, M. L. (1975) Heme A of cytochrome *c* oxidase: Structure and properties comparisons with hemes B, C, and S and derivatives, *J. Biol. Chem. 250*, 7602−7622.
39. Fuhrhop, J.-H., and Smith, K. M. (1975) in *Porphyrins and metalloporphyrins* (Smith, K. M., Ed.) pp 757−869, Elsevier, Amsterdam.
40. Paul, K.-G. (1950) The splitting with silver salts of the cysteine-porphyrin bonds in cytochrome, *Acta Chem. Scand. 4*, 239−244.
41. Ambler, R. P. (1963) The amino acid sequence of *Pseudomonas* cytochrome *c*-551, *Biochem. J. 89*, 349−378.
42. Carpena, X., Loprasert, S., Mongkolsuk, S., Switala, J., Loewen, P. C., and Fita, I. (2003) Catalase-peroxidase KatG of *Burkholderia pseudomallei* at 1.7 Å resolution, *J. Mol. Biol. 327*, 475−489.
43. Ames, J. M. (1994) in *Sulfur compounds in foods*, pp 147−159, American Chemical Society, Washington, DC.
44. Cole, K. C., Sandorfy, C., Fabi, M. T., Olivato, P. R., Rittner, R., Trufem, C., Viertler, H., and Wladislaw, B. (1977) Interaction between the carbonyl group and a sulfur atom. Part 8. Correlation between the basicity constants, corrected for steric effects, and Taft s* values for some ketones and nitriles, *J. Chem. Soc., Perkin Trans. 2*, 2025−2027.
45. Olivato, P. R., and Guerrero, S. A. (1990) Conformational and electronic interaction studies of α-substituted carbonyl compounds. Part 9. ω-Hetero-substituted acetophenones, *J. Chem. Soc., Perkin Trans. 2*, 465−471.
46. Angell, R. M., Biggadike, K., Farrell, R. M., Flack, S. S., Hancock, A. P., Irving, W. R., Lynn, S. M., and Procopiou, P. A. (2002) Novel glucocorticoid antedrugs possessing a 21-(γ-lactone) ring, *J. Chem. Soc., Perkin Trans. 1*, 831−839.
47. Smith, K. M. (1975) *Porphyrins and Metalloporphyrins*, pp 910, Elsevier, Amsterdam.
48. Scheidt, W. R., and Reed, C. A. (1981) Spin-state/stereochemical relationships in iron-porphyrins: implications for the hemoproteins, *Chem. Rev. 81*, 543−555.
49. Makinen, M. W., and Churg, A. K. (1983) in *Iron Porphyrins* (Lever, A. B. P., and Gray, H. B., Eds.) pp 141−235, Addison-Wesley, Reading, MA.
50. Scott, R. A., and Mauk, A. G. (1996) *Cytochrome C: A Multidisciplinary Approach*, pp 728, University Science Books, Sausalito, CA.
51. Reddy, K. S., Angiolillo, P. J., Wright, W. W., Laberge, M., and Vanderkooi, J. M. (1996) Spectral splitting in the α ($Q_{0,0}$) absorption band of ferrous cytochrome *c* and other heme proteins, *Biochemistry 35*, 12820−12830.
52. Rasnik, I., Sharp, K. A., Fee, J. A., and Vanderkooi, J. M. (2001) Spectral analysis of cytochrome *c*: Effect of heme conformation, axial ligand, peripheral substituents and local electric fields, *J. Phys. Chem. B 105*, 282−286.
53. Shelnutt, J. A. (1980) The Raman excitation spectra and absorption spectrum of a metalloporphyrin in an environment of low symmetry, *J. Chem. Phys. 72*, 3948−3958.
54. Lemberg, M. R. (1969) Cytochrome oxidase, *Physiol. Rev. 49*, 48−121.
55. Marzocchi, M. P., and Smulevich, G. (2003) Relationship between heme vinyl conformation and the protein matrix in peroxidases, *J. Raman Spectrosc. 34*, 725−736.
56. Blauer, G., Sreerama, L., and Woody, R. W. (1993) Optical activity of hemoproteins in the Soret region. Circular dichroism of the heme undecapeptide of cytochrome *c* in aqueous solution, *Biochemistry 32*, 6674−6679.
57. Hsu, M. C., and Woody, R. W. (1971) The origin of the heme Cotton effects in myoglobin and hemoglobin, *J. Am. Chem. Soc. 93*, 3515−3525.
58. Wittung-Stafshede, P. (1998) A stable, molten-globule-like cytochrome *c*, *Biochim. Biophys. Acta 1382*, 324−332.
59. Spiro, T. G. (1985) Resonance Raman spectroscopy as a probe of heme protein structure and dynamics, *Adv. Protein Chem. 37*, 111−159.
60. Kihara, H., Hon-nami, K., and Kitagawa, T. (1978) Alkaline isomerization of thermoresistant cytochrome c_{552} and horse heart cytochrome *c* studied by absorption and resonance Raman spectroscopy, *Biochim. Biophys. Acta 532*, 337−346.
61. Hon-nami, K., Kihara, T., Kitagawa, T., Miyazawa, T., and Oshima, T. (1980) Proton nuclear magnetic resonance and resonance Raman studies of thermophilic cytochrome c_{552} from *Thermus thermophilus* HB8, *Eur. J. Biochem. 110*, 217−223.
62. Abe, M., Kitagawa, T., and Kyogoku, Y. (1978) Resonance Raman spectra of octaethylporphinato-Ni(II) and *meso*-deuterated and ^{15}N substituted derivatives. II. A normal coordinate analysis, *J. Chem. Phys. 69*, 4526−4534.
63. Hu, S., Morris, I. K., Singh, J. P., Smith, K. M., and Spiro, T. G. (1993) Complete assignment of cytochrome *c* resonance Raman spectra via enzymatic reconstitution with isotopically labeled hemes, *J. Am. Chem. Soc. 115*, 12446−12458.
64. Salmeen, I., Rimai, L., and Babcock, G. (1978) Raman spectra of heme A, cytochrome oxidase−ligand complexes, and alkaline denatured oxidase, *Biochemistry 17*, 800−806.
65. Bocian, D. F., Masthay, M. B., and Birge, R. R. (1986) Effects of mono- versus di-substitution of conjugating groups on the electronic structure of porphyrins, *Chem. Phys. Lett. 125*, 467−472.
66. Chang, C. K., Hatada, M. H., and Tulinsky, A. (1983) Synthesis and molecular structure of formylporphyrin. Intrinsic properties of porphyrin *a*, *J. Chem. Soc., Perkin Trans.*, 371−378.
67. Reid, L. S., Lim, A. R., and Mauk, A. G. (1986) Role of heme vinyl groups in cytochrome b_5 electron transfer, *J. Am. Chem. Soc. 108*, 8197−8201.
68. Kalsbeck, W. A., Ghosh, A., Pandey, R. K., Smith, K. M., and Bocian, D. F. (1995) Determinants of the vinyl stretching frequency in protoporphyrins. Implications for cofactor-protein interactions in heme proteins, *J. Am. Chem. Soc. 117*, 10959−10968.
69. Babcock, G. T. (1988) in *Biological Applications of Raman Spectroscopy* (Spiro, T. G., Ed.) pp 294−346, John Wiley & Sons, New York.
70. Tsubaki, M., Nagai, K., and Kitagawa, T. (1980) Resonance Raman spectra of myoglobins reconstituted with spirographis and iso-spirographis hemes and iron 2,4-diformylprotoporphyrin IX. Effect of formyl substitution at the heme periphery, *Biochemistry 19*, 379−385.
71. Lutz, M. (1977) Antenna chlorophyll in photosynthetic membranes: a study by resonance Raman spectroscopy, *Biochim. Biophys. Acta 460*, 408−430.
72. Ching, Y., Argade, P. V., and Rousseau, D. L. (1985) Resonance Raman Spectra of CN^--Bound Cytochrome Oxidase: Spectral Isolation of Cytochromes a^{2+}, $a_3{}^{2+}$, and $a_3{}^{2+}(CN^-)$, *Biochemistry 24*, 4938−4946.
73. Oertling, W. A., Surerus, K. K., Einarsdottir, O., Fee, J. A., Dyer, R. B., and Woodruff, W. H. (1994) Spectroscopic characterization of cytochrome ba_3, a terminal oxidase from *Thermus thermophilus*: Comparison of the a_3/Cu_B site to that of bovine cytochrome aa_3, *Biochemistry 33*, 3128−3141.
74. La Mar, G. N., Satterlee, J. D., and de Ropp, J. S. (2000) in *The Porphyrin Handbook* (Kadish, K. M., Smith, K. M., and Ruilard, R., Eds.) pp 185−298, Academic Press, New York.
75. Kolczak, U., Hauksson, J. B., Davis, N. L., Pande, U., de Ropp, J. S., Langry, K. C., Smith, K. M., and La Mar, G. N. (1999) ^1H NMR investigation of the role of intrinsic heme versus protein-induced rhombic perturbations on the electronic structure of low-spin ferrihemoproteins: Effect of heme substituents on heme orientation in myoglobin, *J. Am. Chem. Soc. 121*, 835−843.
76. Shokhirev, N. V., and Walker, F. A. (1998) The effect of axial ligand plane orientation on the contact and pseudocontact shifts of low-spin ferriheme proteins, *J. Biol. Inorg. Chem. 3*, 581−594.
77. Soulimane, T., von Walter, M., Hof, P., Than, M. E., Huber, R., and Buse, G. (1997) Cytochrome c_{552} from *Thermus thermophilus*: A functional and crystallographic investigation, *Biochem. Biophys. Res. Commun. 237*, 572−576.
78. Fischer, H., and von Seeman, C. (1936) Die Konstitution des Spirographhishämins, *Z. Physiol. Chem. 242*, 133−157.
79. Morrison, R. T., and Boyd, R. N. (1992) *Organic Chemistry*, 6th ed., Prentice Hall, Englewood Cliffs, NJ.
80. Lightner, D. A., McKonagh, A. F., Wijekoon, W. M. D., and Reisinger, M. (1988) Amplification of optical activity by remote chiral functionality. Circular dichroism of bilirubin *exo*-vinyl *N*-acetyl-L-cysteine adducts, *Tetrahedron Lett. 29*, 3507−3510.
81. Hanson, R. M. (2003) in *Organic Reactions* (Overman, L. E., Ed.) pp 1−160, John Wiley & Sons, New York.

82. Branalt, J., Kvarnstrom, I., Classon, B., and Samuelsson, B. (1996) Synthesis of [4,5-bis(hydroxymethyl)-1,3-oxathiolan-2-yl]nucleosides as potential inhibitiors of HIV vis stereospecific base-induced rearrangement of a 2,3-epoxy thioacetate, *J. Org. Chem. 61*, 3604−3610.
83. Claiborne, A., Miller, H., Parsonage, D., and Ross, R. P. (1993) Protein-sulfenic acid stabilization and function in enzyme catalysis and gene regulation, *FASEB J. 7*, 1483−1490.
84. Barker, P. D., Ferrer, J. C., Mylrajan, M., Loehr, T. M., Feng, R., Konishi, Y., Funk, W. D., MacGillivray, R. T. A., and Mauk, A. G. (1993) Transmutation of a heme protein, *Proc. Natl. Acad. Sci. U.S.A. 90*, 6542−6546.
85. Salmeen, A., Jannik, N., Andersen, J. N., Myers, M. P., Meng, T.-C., Hinks, J. A., Tonks, N. K., and Barford, D. (2003) Redox regulation of protein tyrosine phosphatase 1B involves a sulphenyl-amide intermediate, *Nature 423*, 769−773.
86. Keck, G. E., Cressman, E. N. K., and Enholm, E. J. (1989) Intramolecular allystannane cyclizations in alkaloid synthesis: Application to pyrrolizidine alkaloids, *J. Org. Chem. 54*, 4345−4349.
87. Gerlach, B., and Montforts, F.-P. (1995) Azachlorins: Synthesis of a novel type of hydroporphyrins from the bile pigment bilirubin, *Liebigs Ann.*, 1509−1514.
88. Fava, C., Galeazzi, R., Mobbili, G., and Orena, M. (1999) New chiral 3-naphthylaminomethyl-pyrrolidines: an unexpected epimerisation reaction, *Heterocycles 51*, 2463−2470.

BI048968L